



**Discover Generics**

Cost-Effective CT & MRI Contrast Agents

**FRESENIUS  
KABI**

[WATCH VIDEO](#)

**AJNR**

This information is current as  
of June 30, 2025.

## **Changes in Ventricular and Cortical Volumes following Shunt Placement in Patients with Idiopathic Normal Pressure Hydrocephalus**

P.M. Cogswell, M.C. Murphy, M.L. Senjem, H. Botha, J.L. Gunter, B.D. Elder, J. Graff-Radford, D.T. Jones, J.K. Cutsforth-Gregory, C.G. Schwarz, F.B. Meyer, J. Huston III and C.R. Jack, Jr

*AJNR Am J Neuroradiol* 2021, 42 (12) 2165-2171

doi: <https://doi.org/10.3174/ajnr.A7323>

<http://www.ajnr.org/content/42/12/2165>

# Changes in Ventricular and Cortical Volumes following Shunt Placement in Patients with Idiopathic Normal Pressure Hydrocephalus

P.M. Cogswell, M.C. Murphy, M.L. Senjem, H. Botha, J.L. Gunter, B.D. Elder, J. Graff-Radford, D.T. Jones, J.K. Cutsforth-Gregory, C.G. Schwarz, F.B. Meyer, J. Huston III, and C.R. Jack Jr



## ABSTRACT

**BACKGROUND AND PURPOSE:** While changes in ventricular and extraventricular CSF spaces have been studied following shunt placement in patients with idiopathic normal pressure hydrocephalus, regional changes in cortical volumes have not. These changes are important to better inform disease pathophysiology and evaluation for comorbidity. The purpose of this work is to investigate changes in ventricular and cortical volumes in patients with idiopathic normal pressure hydrocephalus following ventriculoperitoneal shunt placement.

**MATERIALS AND METHODS:** This is a retrospective cohort study of patients with idiopathic normal pressure hydrocephalus who underwent 3D T1-weighted MR imaging before and after ventriculoperitoneal shunt placement. Images were analyzed using tensor-based morphometry with symmetric normalization to determine the percentage change in ventricular and regional cortical volumes. Ventricular volume changes were assessed using the Wilcoxon signed rank test, and cortical volume changes, using a linear mixed-effects model ( $P < .05$ ).

**RESULTS:** The study included 22 patients (5 women/17 men; mean age, 73 [SD, 6] years). Ventricular volume decreased after shunt placement with a mean change of  $-15.4\%$  ( $P < .001$ ). Measured cortical volume across all participants and cortical ROIs showed a mean percentage increase of  $1.4\%$  ( $P < .001$ ). ROIs near the vertex showed the greatest percentage increase in volume after shunt placement, with smaller decreases in volume in the medial temporal lobes.

**CONCLUSIONS:** Overall, cortical volumes mildly increased after shunt placement in patients with idiopathic normal pressure hydrocephalus with the greatest increases in regions near the vertex, indicating postshunt decompression of the cortex and sulci. Ventricular volumes showed an expected decrease after shunt placement.

**ABBREVIATIONS:** DESH = disproportionately enlarged subarachnoid space hydrocephalus; HCTS = high-convexity or midline tight sulci; iNPH = idiopathic normal pressure hydrocephalus

Idiopathic normal pressure hydrocephalus (iNPH) is a clinicoradiologic syndrome of gait dysfunction, cognitive decline, and urinary incontinence, with a poorly understood etiology.<sup>1</sup> In recent years, a subtype of iNPH has been described, disproportionately enlarged subarachnoid space hydrocephalus (DESH), characterized by the imaging findings of ventriculomegaly, tight

high-convexity sulci, and enlarged Sylvian fissures.<sup>2–5</sup> DESH is thought to represent morphologic changes related to disordered CSF dynamics and is part of the Japanese criteria for the diagnosis of iNPH.<sup>6</sup>

The symptoms of iNPH, particularly gait impairment, may be treated with CSF diversion, most commonly ventriculoperitoneal shunt placement.<sup>7</sup> Some of the morphologic features of iNPH and, in particular DESH, have also been shown to change after shunt placement. As expected, the ventricles decrease in size following shunt placement.<sup>8,9</sup> Additionally, the supra-Sylvian CSF spaces that are narrowed in patients with DESH increase in size with shunt placement, while the total brain parenchyma has been shown to undergo no change or slight expansion.<sup>9,10</sup>

Although changes in total brain parenchymal volume have been studied after shunt placement,<sup>9</sup> specific changes in cortical volume and how changes vary in different brain regions have not. Knowledge of changes in cortical volume is of interest to provide


Received May 22, 2021; accepted after revision August 18.

From the Departments of Radiology (P.M.C., M.C.M., J.L.G., C.G.S., J.H., C.R.J.), Information Technology (M.L.S.), Neurology (H.B., J.G.-R., D.T.J., J.K.C.-G.), Neurosurgery (B.D.E., F.B.M.), and Biomedical Engineering (B.D.E.), Mayo Clinic, Rochester, Minnesota.

This work was supported by the Theodore W. Batterman Family Foundation.

Paper previously presented, in part, at: Annual Meeting of the American Society of Neuroradiology, May 20 to June 4, 2020; Virtual.

Please address correspondence to Petrice M. Cogswell, MD, PhD, Mayo Clinic, 200 First St SW, Rochester, MN 55902; e-mail: Cogswell.petrice@mayo.edu

 Indicates article with online supplemental data.

<http://dx.doi.org/10.3174/ajnr.A7323>

further insight into morphometric disease-related changes and to better inform evaluation of cortical volumes in iNPH. We hypothesized that with decreases in ventricular volume after shunt placement, cortical volumes would increase secondary to decreased mass effect or crowding of the sulci at the vertex. We sought to investigate changes in ventricular volumes and regional changes in cortical volume in patients with iNPH following shunt placement.

## **MATERIALS AND METHODS**

### **Patients**

Patients with a diagnosis of iNPH and MR imaging with 3D T1WI performed before and after ventriculoperitoneal shunt placement from July 2015 through January 2021 were identified retrospectively. Patients were excluded if the 3D T1WI was not performed on a machine from the same MR imaging vendor, with the same field strength before and after shunt placement. Patients with suspected secondary hydrocephalus (eg, congenital outflow obstruction or prior intracranial intervention) based on imaging findings and review of the medical history were excluded. The study was performed under institutional review board approval.

### **MR Imaging**

Imaging was performed on a 1.5T or 3T scanner (GE Healthcare) with a standard 8-channel head coil; by design, the field strength remained constant for each patient. Both 1.5T and 3T data were included because these field strengths have been shown to provide similar and reliable results for the morphometric analyses described below, as long as the field strength is constant within each individual. The 3D T1WI was performed with an MPRAGE sequence with the following 3T acquisition parameters: TR/TE = 6.3/2.6 ms, TI = 900 ms, FOV =  $260 \times 260$  mm<sup>2</sup>, matrix =  $256 \times 256$ , section thickness = 1.2 mm, sensitivity encoding  $R_y = 2$ . Acquisition parameters for 1.5T MPRAGE were TR/TE = 10.0/4.1 ms, TI = 1000 ms, FOV =  $240 \times 240$  mm<sup>2</sup>, matrix =  $192 \times 192$ , section thickness = 1.2 mm. If multiple imaging examinations were available, the MR imaging examination performed before and nearest to the date of shunt placement was chosen as the pre-shunt MR imaging examination. All eligible postshunt MR imaging examinations were included.

### **Qualitative Assessment for HCTS**

Because we hypothesized that cortical volume would increase after shunt placement secondary to the resolution of mass effect from high-convexity or midline tight sulci (HCTS), a feature of DESH, the presence of HCTS was qualitatively determined. Two readers (P.M.C., J.G.R.) individually reviewed the pre-shunt MR imaging examinations for each patient to determine whether HCTS was present. Disagreement was settled by consensus review.

### **Measurement of Ventricular and Cortical Volume Changes**

Tensor-based morphometry with symmetric normalization<sup>11</sup> was used to determine the percentage change in ventricular and regional cortical volumes between MR imaging examinations for each patient. In this technique, all possible pairs of MR imaging

examinations for a patient are coregistered and warped to each other to reduce measurement variability, improve accuracy in longitudinal measurements, and allow improved power to detect more subtle changes compared with an analysis of independently calculated volume measurements for each time point.<sup>11–13</sup> Before analysis, quality control was performed to exclude examinations with motion or failed segmentation.

For the tensor-based morphometry with symmetric normalization analysis, first, each T1WI was run through the statistical parametric mapping (SPM12; <http://www.fil.ion.ucl.ac.uk/spm/software/spm12>) unified segmentation<sup>14</sup> pipeline to obtain tissue (gray matter, white matter, and CSF) segmentations as well as bias-corrected gray-scale images. For each patient, all included T1WI was rigidly coregistered to that patient's common mean using SPM12 and run through an in-house-developed differential bias-correction algorithm. The differential bias-correction algorithm-processed images were once again registered to their mean and resampled to 1-mm isotropic resolution. For each pair of MR imaging dates, the "MR imaging late" image was warped to the "MR imaging early" image, and the "MR imaging early" to "MR imaging late" image using Advanced Normalization Tools (ANTs) software (<http://picsl.upenn.edu/software/ants/>)<sup>15</sup> to derive a symmetric nonlinear deformation, which defines a mapping between the 2 images. These deformations were applied in each direction, and the resulting warped images were averaged with their original counterparts to create a "synthetic early" and a "synthetic late" image. An image of the log-transformed Jacobian determinants or voxelwise measure of local expansion or contraction of volume was formed for the deformation in each direction, and the synthetic early and synthetic late images were each run through SPM12 unified segmentation to get revised tissue probability maps in both the early and late image domains. The log-transformation (natural logarithm) of the Jacobian determinants was used for display purposes because it centers change about zero with values that approximately correspond to the percentage change.

The ventricles and cortical regions were segmented on the basis of the MCALT ADIR122 atlas (<https://www.nitrc.org/projects/mcalt/>),<sup>16</sup> by warping the MCALT template to the space of each early and late image. The ventricle atlas included the lateral and third ventricles. The cortex was parcellated into 43 regions (Online Supplemental Data) in each cerebral hemisphere for a total of 86 regions. Including only gray matter and CSF voxels for cortical and ventricle regions, respectively, the log-Jacobian images were parcellated into individual ROIs, and the mean log-Jacobian was computed within each ROI. For each ROI, the mean log-Jacobian value from the "late to early" deformation was averaged with the inverse of the log-Jacobian value in the "early to late" direction to estimate regional percentage change in volume. For primary analyses, the comparison of change between the pre-shunt MR imaging and the last available postshunt MR imaging was used. Surf Ice (<https://www.nitrc.org/projects/surfire/>) was used to visualize regional cortical volume changes.

### **Change in Ventricular and Cortical Volumes with Time**

To evaluate the temporal profile of ventricular and cortical volume changes, we plotted the percentage change versus time. For

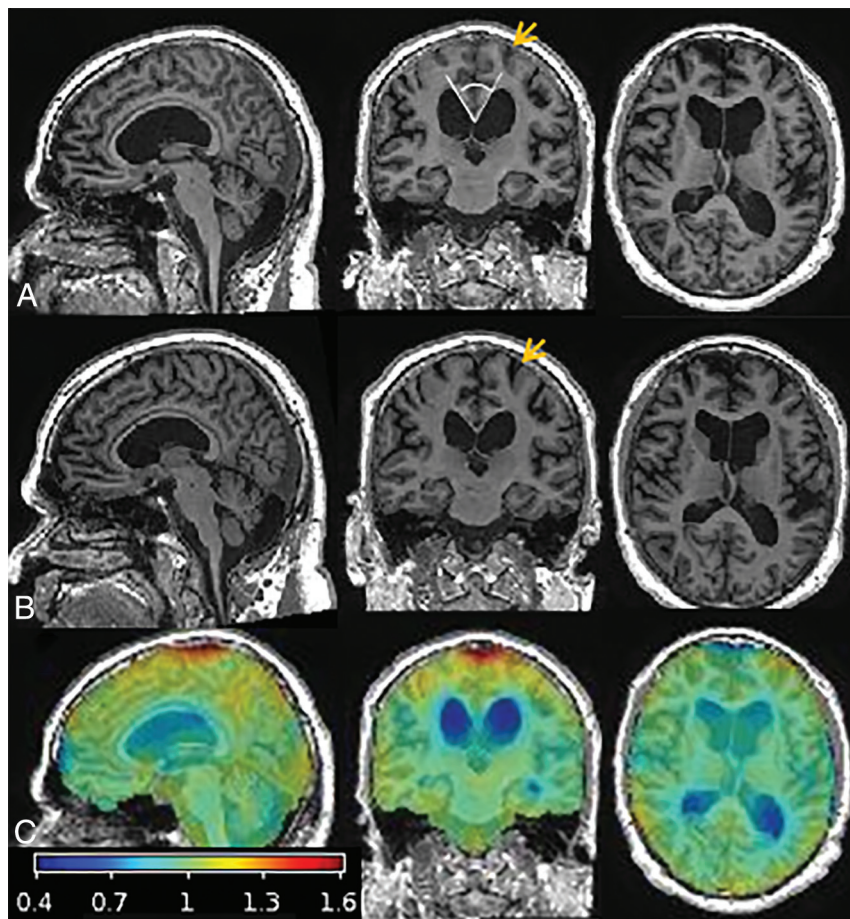


**FIG 1.** T1-weighted MR imaging and overlaid Jacobian maps of estimated changes between pre- and postshunt imaging for a representative patient, a 66-year-old man with INPH. Sagittal, coronal, and axial slices of pre- (A) and postshunt (B) T1WI after registration to the patient's common mean and differential bias correction. C, Map of voxelwise Jacobian determinants overlaid on the preshunt T1WI to demonstrate changes that occurred after shunt placement by warping the late-to-early image: The ventricles contracted (blue) and CSF spaces at the vertex and surrounding parenchyma expanded (red and orange). Although changes in parenchymal volume are not visibly apparent on the T1WI, the coronal images demonstrate decreased crowding of the sulci at the vertex after shunt placement (orange arrows), corresponding to regions that showed an increase in cortical volume after shunt placement. The callosal angle measurement is demonstrated in the coronal image in row A (white lines).

these analyses, the date of the shunt placement was considered to be time zero because it is assumed that the volume changes being assessed are primarily the effect of shunt placement and that no discernible changes occurred in the patient's ventricle size or cortical volume from the date of the preshunt MR imaging to the date of shunt placement. The time (months) for each postshunt MR imaging was calculated as the time between shunt placement and the MR imaging examination. For this analysis, the calculated percentage change between each sequential set of MR imaging examinations was used.

To evaluate the degree of change that occurs in ventricular and gray matter volume in the first few months after shunt placement versus those that occur later, we computed the change in volume that occurred between the preshunt MR imaging and postshunt MR1 and the change between postshunt MR1 and MR2 in patients with 2 postshunt MR imaging examinations.

### Posterior Callosal Angle

As a secondary analysis, the posterior callosal angle was evaluated because it is a more widely accessible and studied measure than ventricular volume, with an angle  $<90^\circ$  considered suggestive of INPH.<sup>17</sup> The posterior corpus callosal angle was measured on the T1WI using a multiplanar reformatting tool (Visage, Version 7.1.14; Visage Imaging) as previously described<sup>8,17</sup> and is demonstrated in Fig 1A. The pre- and postshunt T1WI were coregistered. The anterior/posterior commissure plane was identified in the sagittal plane, and the callosal angle was measured on the coronal image perpendicular to the anterior/posterior commissure plane line at the posterior commissure for each of the pre- and postshunt images.

### Statistical Analyses

Analyses were performed in Matlab (Version R2018a; MathWorks). A linear mixed-effects model was used to test for a significant change in cortical volume in the set of ROIs spanning the cerebral cortex. A 1-sided Wilcoxon signed rank test was used to evaluate a decrease in ventricular volume and an increase in the posterior callosal angle between the preshunt and latest MR imaging examination. For patients with 2 postshunt MR imaging examinations, the difference in volume changes between the preshunt and postshunt MR1 and the postshunt MR1 to postshunt MR2 was assessed using the Wilcoxon matched pairs signed rank test. Percentage change in ventricular and cortical volumes was summarized for patients with-

versus-without HCTS, but statistical analysis was not performed due to low number of patients in the "without HCTS" group.

Pair-wise comparisons of associations in imaging metrics were assessed using the Spearman correlation. We evaluated the following associations: percent change in ventricular volume versus mean percent change in cortical volume, percent change in ventricular volume versus change in callosal angle, and change in callosal angle versus mean percent change in cortical volume.

Additional analyses were performed to assess the effect of shunt valve type and location on volume measurements. The Wilcoxon rank sum test was used to assess differences in ventricular volume and mean cortical volume change between patients with Codman Certas Plus (Integra LifeSciences) and Delta (Medtronic) valves and to compare cortical volume changes in the right-versus-left cerebral hemisphere for each cortical region,



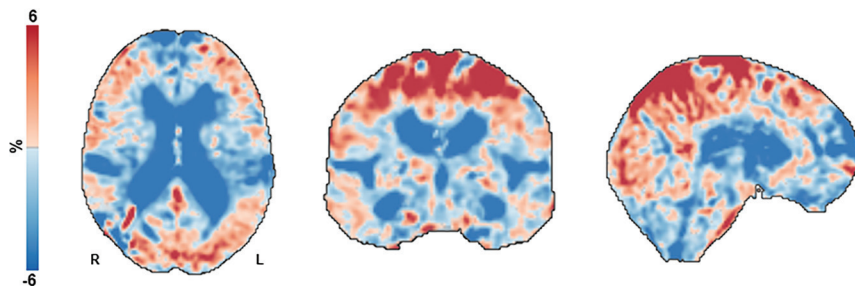


**FIG 2.** Voxelwise maps of estimated mean percentage change in volume from pre- to postshunt MR imaging across all patients. Axial, coronal, and sagittal slices of the mean estimated percentage change in volume (log-Jacobian, which is centered at zero) for all voxels within the total intracranial volume mask. In this display, the tissue class (CSF, gray matter, white matter) is not considered. After shunt placement, there was an expansion or increase in CSF and parenchymal volumes primarily near midline at the vertex (red). Contraction or decrease in volume occurred in the ventricles, extraventricular CSF spaces such as the Sylvian fissures, and anterior-inferior frontal and temporal convexities (blue).

because all patients had a right-sided shunt placement. For all statistical tests,  $P < .05$  was considered significant.

## RESULTS

### Patients

We identified 26 patients with eligible pre- and postshunt MR imaging examinations. Two patients were excluded due to suspected secondary hydrocephalus in the setting of prior craniotomy for tumor resection. Two patients with iNPH were excluded, one due to image motion and one due to failed tissue-class assignment on the preshunt MR imaging examination. The study, thus, included 22 patients (5 women/17 men; mean age, 73 [SD, 6] years; range, 61–84 years). Preshunt MR imaging was performed, on average, 2.0 (SD, 2.4) months before shunt placement. There were 17 patients with 1 postshunt MR imaging examination, and the other 5 had 2 postshunt MR imaging examinations. With the date of shunt placement as time zero, the latest postshunt imaging was performed, on average, 7.0 (SD, 7.0) months (range, 1–25 months) after shunt placement. Although robust clinical metrics suitable for research purposes were not consistently available in this cohort, 20/22 patients reported sustained improvement in at least one of the clinical domains of gait, cognition, and incontinence during imaging follow-up.

### Global Volume Changes

Pre- and postshunt T1WI with overlaid Jacobian determinant maps are shown for a representative patient in Fig 1. The estimated mean voxelwise percentage change in volume (log-Jacobian) from pre- to postshunt MR imaging among all patients is shown in Fig 2; the scale is compressed relative to the Jacobian maps in Fig 1, to better show regional parenchymal changes. The voxelwise maps demonstrated the global changes that occurred after shunt placement throughout the brain parenchyma, ventricles, and CSF spaces, including regions not specifically evaluated in regional analyses. The CSF spaces and parenchyma near the midline vertex expanded after shunt placement. The ventricles and Sylvian fissures contracted after shunt placement, and

there were regions of parenchymal contraction at the anterior-inferior frontal and temporal lobes.

### Percentage Change in Ventricular Volume

The mean percentage change in ventricular volumes across all patients was  $-15.4\%$  (SD,  $9.4\%$ ) ( $P < .001$ ), while the degree of ventricular volume change varied among patients with a range of  $1.1\%$ – $41.5\%$  (Fig 3). For those patients with 2 postshunt follow-up MR imaging examinations ( $n = 5$ ), there was a continued decrease in ventricular volume during the 2 examinations. On average, the mean percentage change in ventricular volume was similar between the preshunt MR imaging and the first postshunt examination ( $-9.4\%$

[SD,  $1.3\%$ ] at a mean of 2.1 [SD,  $0.9$ ] months), and in the first-to-second postshunt examinations ( $-10.5\%$  [SD,  $6.4\%$ ] from, on average, 3 months to 8.9 [SD,  $3.4$ ] months postshunt;  $P = .81$ ).

### Percentage Change in Cortical Volume

Measured cortical volume across all participants and cortical ROIs showed a statistically significant mean percentage increase of  $1.4\%$  (SD,  $1.3\%$ ) ( $P < .001$ ), with a range in mean cortical volume change among patients of  $-2.3\%$ – $3.7\%$  (Fig 3). Consistent regional variations in percentage change in gray matter volume were seen in patients (Fig 4 and Online Supplemental Data). ROIs near the vertex showed the greatest increase in volume after shunt placement (eg,  $4.1\%$ – $7.4\%$  at the parietal superior, frontal superior, precuneus, parietal inferior, and paracentral lobule regions). Regions around the CSF spaces in the inferior brain showed, on average, small decreases in cortical volume after shunt placement (eg,  $-1.1\%$  to  $-2.6\%$  in the insula, amygdala, and hippocampal regions).

In the 5 patients with  $>1$  postshunt MR imaging, the mean percentage change in cortical volume showed greater change from time zero (shunt placement) to the first postshunt examination than from the first-to-second postshunt examination, though the differences did not reach statistical significance ( $1.2\%$  [SD,  $1.3\%$ ] versus  $-0.01\%$  [SD,  $1.1\%$ ],  $P = .19$ ). One of these patients showed a small average decrease in cortical volume from pre- to postshunt MR imaging. The other 4 patients showed an overall increase in cortical volume from the preshunt to the first postshunt MR imaging, with smaller, variable degrees of positive and negative changes from the first-to-second postshunt MR imaging. Of the 2 patients with initial increases in cortical volume followed by small decreases in cortical volume, one had a continued decrease in ventricular size from the first-to-second postshunt MRI and one had a relatively stable ventricular size between those time points.

### Shunt Valve

Of the 22 patients, the first 9 had right-frontal-approach Delta 1.0 valve ventriculoperitoneal shunts, and the last 13 had right-parietal-approach Codman Certas Plus programmable valves. Differences in approach and types of shunts were due to the evolving

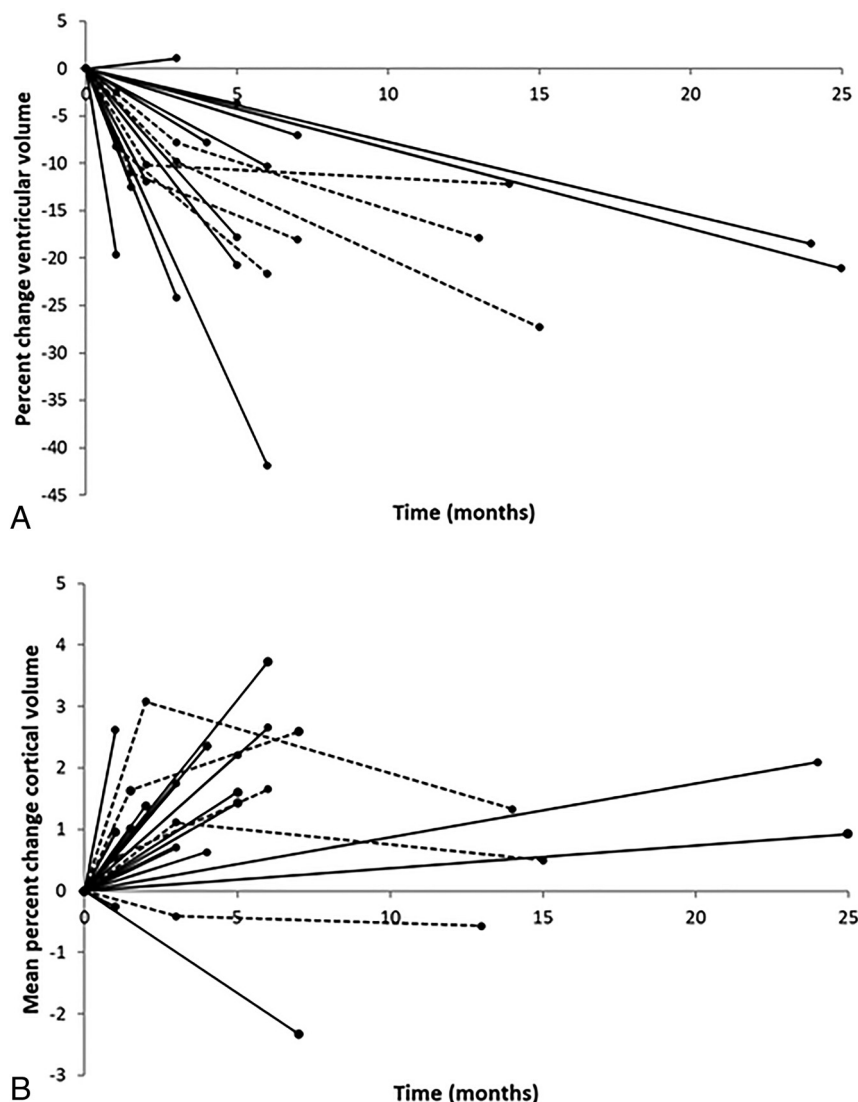


**FIG 3.** Percentage volume change by patient after shunt placement. Percent change in ventricular (A) and mean cortical (B) volume across all ROIs versus time. Each patient is represented by a separate line; patients with 1 postshunt MR imaging are represented by a solid line, and patients with 2 postshunt MRIs are represented by a dotted line. Time zero is the date of shunt placement. In general, ventricular volumes decreased and mean cortical volume increased after shunt placement. In the patients with 2 postshunt MRIs, there was a continued decrease in ventricular volume from postshunt MRI to MR2 and a small variable change in cortical volume during that interval.

neurosurgical practice and surgeon preference. For all patients with the programmable valve, the initial shunt setting was 6, which was chosen as a conservative starting point to avoid overdrainage,<sup>18</sup> and the shunt setting was reduced to 5 within the first several months of follow-up.

The Delta valve did not produce any susceptibility artifacts or obscure adjacent parenchyma. The Codman Certas Plus valve caused susceptibility artifacts that occurred primarily in a portion of the image that was not classified as gray matter, with the exception of the right-inferior and mid-occipital and cerebellar regions, which are not of primary focus in the results of this study. There were no cases of failed processing secondary to shunt-related artifacts.

After excluding the right-inferior and midoccipital regions, which were obscured by artifacts in patients with the Codman Certas Plus valve, there was no statistically significant difference between the right and left sides for any of the cortical regions. Patients with a Codman Certas valve and a Delta valve showed similar changes in mean ventricular ( $-15.0\%$  [SD,  $10.3\%$ ] and  $-15.9\%$  [SD,  $8.6\%$ ], respectively,  $P = .64$ ) and cortical volumes ( $1.2\%$  [SD,  $1.0\%$ ] and  $-1.5\%$  [SD,  $1.5\%$ ], respectively,  $P = .50$ ).

### Qualitative Assessment of HCTS

The readers agreed on the presence or absence of HCTS and judged HCTS to be present on the preshunt MR imaging examination in 20/22 (91%) patients. The 2 participants on which readers disagreed had ventriculomegaly with midline and convexity sulci that were relatively narrowed though not effaced. Although statistical comparison was not performed between patients with-versus-without HCTS due to the low number, on average, those without HCTS showed less change in ventricular and cortical volumes than those with HCTS (mean ventricular volume,  $-9.8\%$  [SD,  $3.0\%$ ] versus  $-15.9\%$  [SD,  $9.7\%$ ] and mean cortical volume change,  $1.0\%$  [SD,  $0.5\%$ ] versus  $1.4\%$  [SD,  $1.4\%$ ]).

### Change in Callosal Angle

The callosal angle, on average, increased by a mean of  $16.4^\circ$  (SD,  $11.8^\circ$ ) ( $P < .001$ ) after shunt placement ( $69.0^\circ$  [SD,  $19.7^\circ$ ] preshunt to  $85.4^\circ$  [SD,  $20.6^\circ$ ] postshunt).

### Association between Changes in Imaging Metrics

The mean cortical volume increased with decreases in ventricular volume ( $\rho = -0.44$ ,  $P = .04$ ). The change in callosal

angle was not as strongly associated with the mean percentage change in cortical volume ( $\rho = 0.21$ ,  $P = .34$ ). The callosal angle increased (or normalized) with a decrease in ventricular volume, though the association of these metrics did not reach statistical significance ( $\rho = -0.40$ ,  $P = .06$ ). These associations are shown in the Online Supplemental Data.

## DISCUSSION

We investigated changes in ventricular and regional cortical volumes after ventriculoperitoneal shunt placement in patients with iNPH. Along with decreases in ventricular volumes after shunt placement, there were changes in cortical volumes, with the

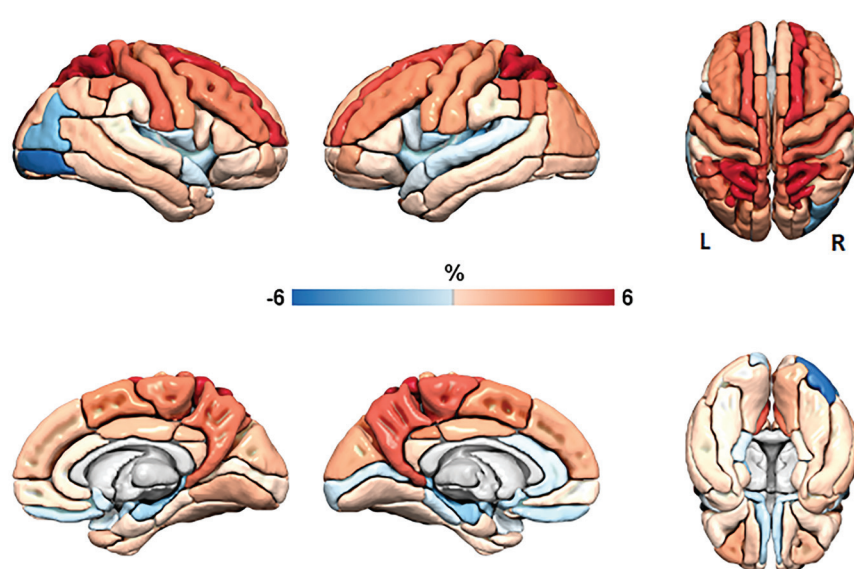


**FIG 4.** Regional cortical mean percentage volume change. Surface-renderings of mean percentage change in cortical volume among all participants by cortical region in the ADIRI22 atlas. These data are a subset of the data shown in Fig 2, considering only voxels determined to be cortical gray matter and demonstrating ROI-wise results, the main analytic method used in this work. Red indicates an increase in volume or expansion from pre- to postshunt MR imaging examinations and is primarily present at the midline vertex regions. Blue indicates a decrease in volume or contraction and is seen adjacent to the temporal horns and Sylvian fissures as well as related to Codman Certas Plus valve artifacts (right occipital). The *first column* shows right-hemisphere lateral and medial views. The *second column* shows left-hemisphere lateral and medial views. The *third column* shows top and bottom views.

greatest increases in cortical volume at regions near the midline vertex.

The ventricles showed an anticipated decrease in size after shunt placement. The mean percentage decrease in ventricular volume of 15% in this study was similar to approximately 14% at 3–8 months after shunt placement in the study by Virhammar et al.<sup>8</sup> Ventricular volume changes occurred within the first few months after shunt placement, and in the subgroup of patients with multiple MR imaging examinations, there was a continued decrease in ventricular volume on subsequent imaging performed several months later. This time course of ventricular volume changes is similar to that described by Yamada et al.<sup>9</sup>

The posterior callosal angle showed a significant increase after shunt placement, as seen in prior studies.<sup>8,9</sup> The association of the change in callosal angle with the percentage change in cortical volume was not as strong as the association of the percentage change in ventricular volume with the percentage change in cortical volume. These findings support volumetric rather than linear measures of anatomy as more robust indicators of disease and treatment-related changes.<sup>9,19</sup>

The mean cortical volume across the cerebral cortex increased after shunt placement, though changes were topographically variable. The greatest increase in cortical volume occurred near the midline vertex, where although not quantified in this study, there was also expansion of the CSF spaces. These are the regions of sulcal effacement in patients presenting with iNPH, and, in particular, patients with DESH. Narrowing of the sulci in the midline vertex regions is associated with compression of the adjacent

cortex. After shunt placement, the ventricles decrease in size, vertex CSF spaces expand, mass effect on the parenchyma lessens, and cortical volumes increase. The enlarged intra- and extra-ventricular CSF spaces and compression of the cortex in patients with iNPH and DESH may be misinterpreted as atrophy and has been termed “pseudoatrophy.”<sup>20</sup>

In this study, we showed that these findings are, at least in part, reversed after CSF diversion. Of note, neither DESH nor HCTS was required for inclusion in this study, nor is it required for a diagnosis of iNPH and shunt placement, but HCTS was present in all except 2 patients. These 2 patients without HCTS had lower-than-average post-shunt changes in ventricular and cortical volumes. The number of patients in this study did not allow subgroup analyses comparing patients with-versus-without HCTS, other features of DESH, or the degree of DESH-like features, though such analyses would be of interest in future work.

While there was an increase in regional cortical volume near the vertex, regional cortical volume in the inferior

aspect of the cerebral hemispheres, adjacent to contracted CSF spaces, showed a decrease in cortical volume after shunt placement. The etiology of these changes is likely multifactorial. Volume decreases may be due, in part, to partial volume effects from the adjacent contracting CSF spaces, given the relatively small size of the affected ROIs. Although iNPH and shunt placement are the primary drivers of morphologic changes for these patients in the study time period, a small and likely negligible degree of regional age-related cortical volume loss (which would affect temporal-limbic areas more than the cortex at the vertex) is possible.<sup>21</sup> Additionally, small changes (ie, on the order of <1%) could be due to variability in longitudinal measurements, as has been seen in prior work.<sup>11,13</sup>

As in prior work evaluating total brain parenchymal volumes, in the subgroup of patients with 2 postshunt MR imaging examinations, cortical volume changes occurred predominantly in the first few months after shunt placement.<sup>9</sup> This observation is likely due to resolution of mass effect on the parenchyma with decreasing ventricular volume and enlarging vertex CSF spaces. After the vertex CSF spaces have decompressed, further decrease in ventricular size or change in CSF spaces would not be anticipated to have associated cortical volume changes. Small observed cortical volumes for long-term follow-up may be related to variations in CSF dynamics as well as variability in measurement.

Overall, the global CSF space and cortical volume changes observed after shunt placement correspond with improvement in the morphologic features of iNPH and DESH. As these entities have become more widely recognized in community populations<sup>22,23</sup> and



volumetric measurement is more widely applied in the clinical evaluation of cognitive decline, awareness of cortical volume changes associated with CSF dynamics disorders is important, to avoid misinterpretation of mass effect on the cortex or relatively low cortical volume as atrophy secondary to neurodegeneration, which may confound disease categorization and evaluation for copathology in the clinical or research setting.

There are limitations to this study. The spatial resolution varied from 1.0– to 1.2 mm, though we have found volumetric calculations at these resolutions comparable. Due to the retrospective nature and strict requirements that the 3D T1WI acquisitions be performed with the same imaging platform, the number of included patients is moderate. The time of postshunt follow-up imaging varied among patients. Despite these limitations, consistent, statistically significant changes were observed. In the future, standardized follow-up intervals and more patients with multiple postshunt MRIs would be beneficial to better delineate the timeline of morphologic changes that occur. Although it would be interesting to assess associations between imaging and clinical metrics, these patients did not undergo similar rigorous quantitative assessment of relevant clinical indices before and after shunt placement to allow such analyses.

## CONCLUSIONS

We found a decrease in ventricular volume and an overall increase in cortical volume, greatest at the midline vertex, following shunt placement in patients with INPH. Changes in cortical volume appeared to occur predominantly in the first few months after shunt placement, while ventricular volumes continued to decrease on subsequent follow-up. These changes correspond with improvement in the morphologic features of INPH, and, specifically, DESH after CSF diversion. Awareness of the artificial reduction of cortical volumes in the setting of disordered CSF dynamics is important in the assessment for neurodegenerative disease, which may present with similar symptoms to INPH or as copathology.

Disclosure forms provided by the authors are available with the full text and PDF of this article at [www.ajnr.org](http://www.ajnr.org).

## REFERENCES

- Adams RD, Fisher CM, Hakim S, et al. **Symptomatic occult hydrocephalus with normal cerebrospinal-fluid pressure.** *N Engl J Med* 1965;273:117–26 [CrossRef Medline](#)
- Ishikawa M, Yamada S, Yamamoto K. **Early and delayed assessments of quantitative gait measures to improve the tap test as a predictor of shunt effectiveness in idiopathic normal pressure hydrocephalus.** *Fluids Barriers CNS* 2016;13:20 [CrossRef Medline](#)
- Kitagaki H, Mori E, Ishii K, et al. **CSF spaces in idiopathic normal pressure hydrocephalus: morphology and volumetry.** *AJNR Am J Neuroradiol* 1998;19:1277–84 [Medline](#)
- Yamashita F, Sasaki M, Takahashi S, et al. **Detection of changes in cerebrospinal fluid space in idiopathic normal pressure hydrocephalus using voxel-based morphometry.** *Neuroradiology* 2010;52:381–86 [CrossRef Medline](#)
- Hashimoto M, Ishikawa M, Mori E, et al. **Study of INPH on neurological improvement (SINPHONI), Diagnosis of idiopathic normal pressure hydrocephalus is supported by MRI-based scheme: a prospective cohort study.** *Cerebrospinal Fluid Res* 2010;7:18 [CrossRef Medline](#)
- Mori E, Ishikawa M, Kato T, et al. **Japanese Society of Normal Pressure Hydrocephalus. Guidelines for management of idiopathic normal pressure hydrocephalus: second edition.** *Neurol Med Chir (Tokyo)* 2012;52:775–809 [CrossRef Medline](#)
- Toma AK, Papadopoulos MC, Stapleton S, et al. **Systematic review of the outcome of shunt surgery in idiopathic normal-pressure hydrocephalus.** *Acta Neurochir (Wien)* 2013;155:1977–80 [CrossRef Medline](#)
- Virhammar J, Laurell K, Cesarini KG, et al. **Increase in callosal angle and decrease in ventricular volume after shunt surgery in patients with idiopathic normal pressure hydrocephalus.** *J Neurosurg* 2018;130:130–35 [CrossRef Medline](#)
- Yamada S, Ishikawa M, Yamaguchi M, et al. **Longitudinal morphological changes during recovery from brain deformation due to idiopathic normal pressure hydrocephalus after ventriculoperitoneal shunt surgery.** *Sci Rep* 2019;9:17318 [CrossRef Medline](#)
- Hiraoka K, Yamasaki H, Takagi M, et al. **Changes in the volumes of the brain and cerebrospinal fluid spaces after shunt surgery in idiopathic normal-pressure hydrocephalus.** *J Neurol Sci* 2010;296:7–12 [CrossRef Medline](#)
- Vemuri P, Senjem ML, Gunter JL, et al. **Alzheimer's Disease Neuroimaging Initiative. Accelerated vs. unaccelerated serial MRI based TBM-SyN measurements for clinical trials in Alzheimer's disease.** *Neuroimage* 2015;113:61–69 [CrossRef Medline](#)
- Ashburner J, Ridgway GR. **Symmetric diffeomorphic modeling of longitudinal structural MRI.** *Front Neurosci* 2012;6:197 [CrossRef Medline](#)
- Cash DM, Frost C, Iheme LO, et al. **Assessing atrophy measurement techniques in dementia: results from the MIRIAD atrophy challenge.** *Neuroimage* 2015;123:149–64 [CrossRef Medline](#)
- Ashburner J, Friston KJ. **Unified segmentation.** *Neuroimage* 2005;26:839–51 [CrossRef Medline](#)
- Avants BB, Epstein CL, Grossman M, et al. **Symmetric diffeomorphic image registration with cross-correlation: evaluating automated labeling of elderly and neurodegenerative brain.** *Med Image Anal* 2008;12:26–41 [CrossRef Medline](#)
- Schwarz CG, Gunter JL, Ward CP, et al. **The Mayo Clinic adult lifespan template: better quantification across the life span.** *Alzheimers Dement* 2017;13:P792 [CrossRef](#)
- Ishii K, Kanda T, Harada A, et al. **Clinical impact of the callosal angle in the diagnosis of idiopathic normal pressure hydrocephalus.** *Eur Radiol* 2008;18:2678–83 [CrossRef Medline](#)
- Khan QUA, Wharen RE, Grewal SS, et al. **Overdrainage shunt complications in idiopathic normal-pressure hydrocephalus and lumbar puncture opening pressure.** *J Neurosurg* 2013;119:1498–502 [CrossRef Medline](#)
- Crook JE, Gunter JL, Ball CT, et al. **Linear vs volume measures of ventricle size: relation to present and future gait and cognition.** *Neurology* 2020;94:e549–56 [CrossRef Medline](#)
- McCarty AM, Jones DT, Dickson DW, et al. **Disproportionately enlarged subarachnoid-space hydrocephalus (DESH) in normal pressure hydrocephalus misinterpreted as atrophy: autopsy and radiological evidence.** *Neurocase* 2019;25:151–55 [CrossRef Medline](#)
- Jack CR, Petersen RC, Xu Y, et al. **The rate of medial temporal lobe atrophy in typical aging and Alzheimer's disease.** *Neurology* 1998;51:993–99 [CrossRef Medline](#)
- Andersson J, Rosell M, Kockum K, et al. **Prevalence of idiopathic normal pressure hydrocephalus: a prospective, population-based study.** *PLoS One* 2019;14:e0217705 [CrossRef Medline](#)
- Graff-Radford J, Gunter JL, Jones DT, et al. **Cerebrospinal fluid dynamics disorders: relationship to Alzheimer biomarkers and cognition.** *Neurology* 2019;93:e2237–46 [CrossRef Medline](#)